Complex Gaussian quadrature of oscillatory integrals

Alfredo Deaño*   Daan Huybrechs†

March 18, 2008

Abstract

We construct and analyze Gauss-type quadrature rules with complex-valued nodes and weights to approximate oscillatory integrals with stationary points of high order. The method is based on substituting the original interval of integration by a set of contours in the complex plane, corresponding to the paths of steepest descent. Each of these line integrals shows an exponentially decaying behaviour, suitable for the application of Gaussian rules with non-standard weight functions. The results differ from those in previous research in the sense that the constructed rules are asymptotically optimal, i.e., among all known methods for oscillatory integrals they deliver the highest possible asymptotic order of convergence, relative to the required number of evaluations of the integrand.

1 Introduction

Oscillatory integrals most commonly appear in applications in the form of so-called *Fourier-type* integrals. They can be written as

$$I[f] = \int_a^b f(x) \mathrm{e}^{\mathrm{i}\omega g(x)} \, \mathrm{d}x, \tag{1}$$

where ω is a frequency parameter. The functions f and g are usually called the *amplitude* and the *phase* or *oscillator*. The numerical evaluation can be difficult when the parameter ω is large, because in that case the integrand is highly oscillatory. A prohibitively large number of quadrature points is needed if one uses a standard rule such as Gaussian quadrature, or any quadrature method based on (piecewise) polynomial interpolation of the integrand.

On the other hand, the principle of stationary phase [1, 20, 24] establishes that when ω is large, the main contributions to the value of $I[f]$ are found near the following points:

*DAMTP, Centre for Mathematical Sciences. University of Cambridge, UK (ad495@cam.ac.uk)

†Department of Computer Science, Katholieke Universiteit Leuven, Belgium (daan.huybrechs@cs.kuleuven.be)

- The endpoints of the interval of integration, $x = a$ and $x = b$.
- The so-called *stationary points*, where one or more derivatives of g vanish:

$$g^{(j)}(\xi) = 0, \qquad j = 1, \ldots, r-1, \quad \text{but} \quad g^{(r)}(\xi) \neq 0.$$

  Consider for example $g(x) = x^r$ at $x = 0$. We say that the stationary point ξ has *order* $r - 1$.

More precisely, the endpoints produce a contribution to the asymptotic expansion of $I[f]$ in inverse powers of ω of the form

$$S_{a,b}[f] = \sum_{k=0}^{\infty} a_k[f]\,\omega^{-k-1}, \qquad \omega \to \infty,$$

for $f \in C^\infty[a,b]$, where the coefficients a_k depend only on the values of f and its derivatives up to order k at the endpoints a and b. A stationary point ξ of order $r-1$ gives a contribution of the form

$$S_\xi[f] = \sum_{k=0}^{\infty} b_k[f]\,\omega^{-\frac{k+1}{r}}, \qquad \omega \to \infty,$$

where b_k again depends on the values of the function f and its derivatives up to order k at the stationary point ξ, see [13, 15, 22]. The full asymptotic expansion can be obtained by adding these contributions,

$$I[f] \sim S_{a,b}[f] + S_\xi[f], \qquad \omega \to \infty.$$

Although these expansions are generally divergent for a fixed value of ω, the first few terms can give a good approximation to $I[f]$ when ω is large, and these asymptotic ideas have been used as a point of departure for the design of other quadrature rules. For instance, Filon-type methods [15] are based on interpolation of the integrand (and its derivatives) at several points within the interval of integration, including the endpoints and the stationary points, in such a way that not only is the accuracy of the asymptotic series retained for large values of ω, but it is also increased for small ω. Other methods include Levin-type methods [17, 21], that achieve a similar goal by solving an associated differential equation. We refer the reader to [12] for a recent review.

From a computational point of view, these methods depend on the evaluation of f and its derivatives at the endpoints and at the stationary point. They can deliver an absolute error that behaves as $\mathcal{O}(\omega^{-n-1})$, when using derivatives up to order $n-1$ at the endpoints. In the presence of a stationary point of order $r-1$, using the same number of derivatives at the stationary point yields an error that behaves as $\mathcal{O}(\omega^{-\frac{n+1}{r}})$. The information that is used here is exactly the information required to compute the first n terms of the asymptotic expansion. A truncated asymptotic expansion based on this information therefore carries the same asymptotic error.

In the past few decades, it has been observed by several authors, in different fields and with varying degrees of generality, that higher asymptotic accuracy can be obtained using the same number of evaluations of f or any of its derivatives [8, 16, 5, 2]. One such approach was recently analyzed in the general setting of integral (1) in [13]. The approach, which derives from the ideas of the classical method of steepest descent, is the following: subject to the analyticity of the integrand, the interval of integration is substituted by a union of contours on the complex plane, such that along these contours the integrand is non-oscillatory and exponentially decaying. Next, each of these integrals is parameterized in a way that enables their efficient evaluation by means of a Gauss-type quadrature. It turns out that the well known optimal polynomial order of Gauss-rules [6] translates into an optimal asymptotic order in terms of the oscillatory parameter ω. In particular, using n quadrature nodes near the endpoints one obtains an absolute error with asymptotic order $\mathcal{O}(\omega^{-2n-1})$. This means that the asymptotic order is roughly doubled, compared to the methods mentioned above, for the same amount of information. No high order derivatives are needed, though the price to be paid is the evaluation of f at complex nodes and the requirement of analyticity.

Other quadrature rules have been used to deal with exponentially decaying integrands along steepest descent paths. Most notably, the adaptive trapezoidal rule gives good results in integral representations of special functions, see a recent review and examples in [10]. The trapezoidal rule yields exponential convergence in certain settings, making it a popular choice [23]. Yet, as will become evident in the current paper (for example from Theorem 2.2), for integrals of the form (1) it is not the best choice for large ω. The asymptotic properties of oscillatory integrals allow one to gradually decrease the computational effort as the frequency grows. This feature is not exploited by the trapezoidal rule, but it is exploited to the highest extent by the use of carefully crafted Gaussian quadrature rules.

The purpose of this paper is two-fold. First, we systematically extend and generalize the results of [13]. We show and prove that the asymptotic accuracy of a truncated asymptotic expansion can be approximately doubled in all cases, including stationary points of arbitrarily high order of degeneracy. We also show how the asymptotic order of non-Gaussian quadrature approaches can be determined. Second, we illustrate the numerical construction of the Gaussian quadrature rules involved in this approach and the location of the quadrature points. We focus on the integral

$$I[f] := \int_a^b f(x) \mathrm{e}^{\mathrm{i}\omega x^r} \,\mathrm{d}x, \tag{2}$$

with $a < 0$, $b > 0$ and with f analytic in a complex neighbourhood of the interval $[a, b]$. This is the canonical example of an oscillatory integral with a stationary point of order $r - 1$, located at the point $\xi = 0$. The results are later extended to the general integral (1).

The method of [13] has also been extended to multivariate oscillatory integrals in [14]. We note that some, but by no means all, results of the current paper can be generalized to a multivariate setting. An important issue is the lack of a comprehensive theory on the existence of Gaussian cubature rules for multivariate integrals, even in the non-oscillatory case [4].

The structure of the paper is as follows: in §2 we briefly recall the computation of the paths of steepest descent and the decomposition of the oscillatory integral into a sum of four non-oscillatory line integrals. Next, we investigate the construction of Gaussian quadrature rules for each of these complex integrals in §3. Since the weight functions associated to these integrals are in general non-classical, special attention is given to the numerical computation of the corresponding nodes and weights. We provide numerical illustration of the location of these nodes, as well as examples with different functions f. In §4 we explore the possibility of designing one quadrature rule for the two paths that involve the stationary point $\xi = 0$. This leads to a problem of constructing Gauss rules with respect to an indefinite linear functional. The resulting rules are asymptotically optimal. Lastly, in §5 we show how the results extend to the general integral (1).

2 The numerical method of steepest descent

2.1 The paths of steepest descent

We restrict ourselves for the time being to the case $g(x) = x^r$. Given a point $x \in [a, b]$, we define the path of steepest descent $h_x(p)$, parameterized by $p \in [0, P]$, such that the real part of the phase function x^r remains constant along the path. This is achieved by solving the equation

$$h_x(p)^r = x^r + \mathrm{i}p, \tag{3}$$

subject to the condition $h_x(0) = x$, which states that the path $h_x(p)$ originates at the point x. Along this path of steepest descent, an integral with the same integrand as (2) becomes

$$I[f; h_x] = \mathrm{e}^{\mathrm{i}\omega x^r} \int_0^P f(h_x(p)) h_x'(p) \mathrm{e}^{-\omega p} \, \mathrm{d}p.$$

Observe that now the integrand is exponentially decaying and that it is non-oscillatory.

Equation (3) has r different solutions for any point x, given explicitly by

$$h_{x,j}(p) = \mathrm{e}^{2\pi \mathrm{i} \frac{j}{r}} \sqrt[r]{x^r + \mathrm{i}p}, \qquad j = 0, \ldots, r-1.$$

The inverse of the analytic function z^r is a multivalued function, and these r solutions correspond exactly to its r different branches. At the points a and b, with $a < 0$ and $b > 0$, the paths of steepest descent are unambiguously determined by the boundary conditions $h_a(0) = a$ and $h_b(0) = b$. Letting

$$j_1 = \left\lfloor \frac{r}{2} \right\rfloor \qquad \text{and} \qquad j_2 = 0,$$

we find the paths as h_{a,j_1} and h_{b,j_2}.

At the stationary point $\xi = 0$, all solutions $h_{0,j}(p)$ satisfy the boundary condition $h_{0,j}(0) = 0$. Yet, we will consider only the branches j_1 and j_2. This choice is illustrated in Figure 1 for the cases $r = 2$ and $r = 3$. In the jargon of steepest descent literature, this choice means that the path $h_{0,j_1}(p)$ leads into the same *valley* of the integrand as the path at a. In particular, deforming the integration interval $[a, \xi]$ onto the contours $h_{a,j_1}(p)$ and $h_{\xi,j_1}(p)$ is justified by Cauchy's integral theorem – likewise for the interval $[\xi, b]$. We thus arrive at a decomposition of the oscillatory integral (2) as a sum of four contributions, up to exponentially small terms, given from the endpoints together with the stationary point $\xi = 0$ (see [13]):

$$I[f] \sim I[f; h_{a,j_1}] - I[f; h_{\xi,j_1}] + I[f; h_{\xi,j_2}] - I[f; h_{b,j_2}] + \mathcal{O}(\mathrm{e}^{-d\omega}), \qquad (4)$$

when $\omega \to \infty$, with $d > 0$ depending on P and on the distance to the nearest singularity of the function f in the complex plane.

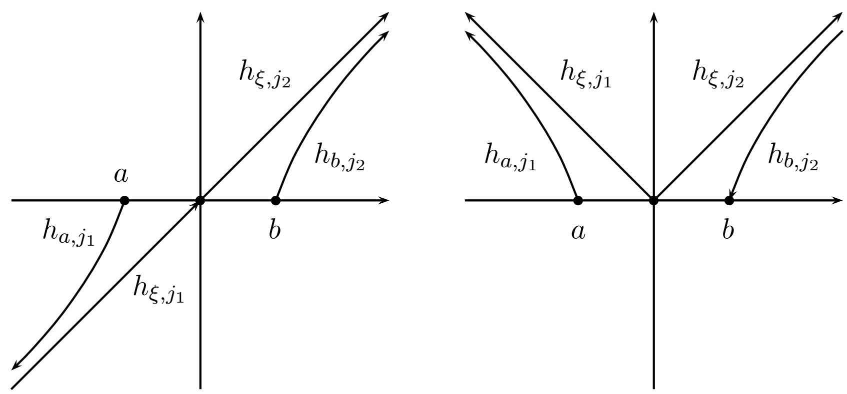

Figure 1: Contours of integration in the complex plane corresponding to even r (left) and odd r (right).

For simplicity of notation, we will consider in the following only the limit case $P = \infty$. For this, it is sufficient that f is analytic in a sufficiently large (and possibly infinitely large) region of the complex plane and that it does not grow faster than exponentially along the paths of steepest descent [13]. All asymptotic results stated further on remain valid if $P < \infty$ is finite. For practical computations, the only restriction is that the quadrature points that we will be computing should lie in the domain of analyticity of both f and g. For sufficiently large ω, this is always the case.

2.2 Numerical evaluation of the line integrals

We have written the integral as a sum of four contributions:

$$
\begin{aligned}
I[f] \sim \mathrm{e}^{\mathrm{i}\omega a^r} \int_0^\infty \phi_{a,j_1}(p)\mathrm{e}^{-\omega p}\,\mathrm{d}p - \int_0^\infty \phi_{\xi,j_1}(p)\mathrm{e}^{-\omega p}\,\mathrm{d}p \\
+ \int_0^\infty \phi_{\xi,j_2}(p)\mathrm{e}^{-\omega p}\,\mathrm{d}p - \mathrm{e}^{\mathrm{i}\omega b^r} \int_0^\infty \phi_{b,j_2}(p)\mathrm{e}^{-\omega p}\,\mathrm{d}p,
\end{aligned}
$$

where for the sake of brevity we use the notation:

$$\phi_{x,j}(p) = f(h_{x,j}(p))h'_{x,j}(p),$$

with $x = a, b$ or ξ and $j = j_1, j_2$. The derivative of the parameterization is given in general by:

$$h'_{x,j}(p) = e^{2\pi\mathrm{i}\frac{j}{r}} \frac{\mathrm{i}}{r}(x^r + \mathrm{i}p)^{-\frac{r-1}{r}}.$$

We will treat the cases of endpoints and stationary points separately.

2.2.1 Line integrals at the endpoints

The line integrals corresponding to the endpoints a and b are well behaved, and their asymptotic expansion can be deduced from Watson's lemma [24]. We have, for example at the point $x = a$,

$$I[f; h_{a,j_1}] \sim \sum_{k=0}^{\infty} a_k \omega^{-k-1},$$

where a_k depends on $f^{(j)}(a)$, $j = 0, \ldots, k$. If one approximates the line integral by truncating the asymptotic expansion after n terms, then the error behaves asymptotically as

$$I[f; h_{a,j_1}] - \sum_{k=0}^{n-1} a_k \omega^{-k-1} = \mathcal{O}(\omega^{-n-1}), \qquad \omega \to \infty. \tag{5}$$

Asymptotic expansions in general may diverge, even if the line integrals involved are well behaved. For any fixed value of ω, the error in (5) may therefore be large and it cannot be decreased reliably by taking additional terms of the expansion. In order to achieve smaller error, it was suggested in [13] to evaluate the line integrals numerically. We are interested, then, in a family of quadrature rules

$$Q[f; h_{a,j_1}] := \sum_{k=1}^{n} w_k(\omega) f(x_k(\omega)), \tag{6}$$

with points $x_k(\omega)$ and weights $w_k(\omega)$ depending on ω, such that

$$I[f; h_{a,j_1}] - Q[f; h_{a,j_1}] = \mathcal{O}(\omega^{-s_n}), \qquad \omega \to \infty. \tag{7}$$

The aim moreover is to maximize the asymptotic order s_n for any given n.

Suitable quadrature rules for the case of endpoints are readily obtained. With the change of variable $q = \omega p$, the line integral $I[f; h_{a,j_1}]$ can be written in the form

$$I[f; h_{a,j_1}] = \mathrm{e}^{\mathrm{i}\omega a^r} \frac{1}{\omega} \int_0^\infty f\left(h_{a,j_1}\left(\frac{q}{\omega}\right)\right) h'_{a,j_1}\left(\frac{q}{\omega}\right) \mathrm{e}^{-q}\,\mathrm{d}q.$$

This form is suitable for the classical Gauss-Laguerre quadrature, i.e. for Gaussian quadrature with the weight function $w(q) = \mathrm{e}^{-q}$. Let w_k^{GL} and x_k^{GL} be the points and weights of an n-point Gauss-Laguerre rule. Then we set

$$x_k(\omega) := h_{a,j_1}\left(\frac{x_k^{GL}}{\omega}\right), \qquad w_k(\omega) := \frac{\mathrm{e}^{\mathrm{i}\omega a^r}}{\omega} h'_{a,j_1}\left(\frac{x_k^{GL}}{\omega}\right) w_k^{GL}. \tag{8}$$

It turns out that the asymptotic order of the approximation is determined by the polynomial order of the Gauss-Laguerre rule.

Lemma 2.1 *Consider a positive number $\alpha \in \mathbb{R}$ and a quadrature rule with n points x_k and weights w_k, such that*

$$\int_0^\infty x^m e^{-x^\alpha}\,\mathrm{d}x = \sum_{k=1}^n w_k x_k^m, \qquad m = 0, \ldots, d-1. \tag{9}$$

If $\int_0^\infty u(x) e^{-\omega x^\alpha}\,\mathrm{d}x$ exists for $\omega \geq \omega_0$ and if u is analytic at $x = 0$, then it is true that

$$\int_0^\infty u(x) e^{-\omega x^\alpha}\,\mathrm{d}x - \omega^{-1/\alpha} \sum_{k=1}^n w_k u(x_k\,\omega^{-1/\alpha}) = \mathcal{O}(\omega^{-\frac{d+1}{\alpha}})$$

when $\omega \to \infty$.

Proof 2.1 *Using the change of variables $x = \omega^{-1/\alpha} t$, we have*

$$\int_0^\infty x^m e^{-\omega x^\alpha}\,\mathrm{d}x = \omega^{-1/\alpha} \sum_{k=1}^n w_k (x_k \omega^{-1/\alpha})^m,$$

for $m = 0, \ldots, d-1$, from the exactness conditions (9).

Since u is analytic at $x = 0$, it has a convergent Taylor series for some $R > 0$,

$$u(x) = \sum_{i=0}^\infty \frac{u^{(i)}(0)}{i!} x^i, \qquad x < R.$$

Denote by $u_d(x) = \sum_{i=0}^{d-1} \frac{u^{(i)}(0)}{i!} x^i$ the Taylor series truncated after d terms and define $u_e(x) := u(x) - u_d(x)$ as the remainder. Letting

$$\mathcal{L}_\omega[u] := \int_0^\infty u(x) e^{-\omega x^\alpha}\,\mathrm{d}x,$$

we have

$$\mathcal{L}_\omega[u] = \mathcal{L}_\omega[u_d] + \mathcal{L}[u_e] = \omega^{-1/\alpha} \sum_{k=1}^{n} w_k u_d(x_k\, \omega^{-1/\alpha}) + \mathcal{L}[u_e].$$

The latter equality is true because the quadrature rule is exact for u_d. It follows that the quadrature error is given by

$$\mathcal{L}[u] - \omega^{-1/\alpha} \sum_{k=1}^{n} w_k u(x_k\, \omega^{-1/\alpha}) = \mathcal{L}[u_e] - \omega^{-1/\alpha} \sum_{k=1}^{n} w_k u_e(x_k\, \omega^{-1/\alpha}).$$

We can bound both terms on the right hand side by $\mathcal{O}(\omega^{-\frac{d+1}{\alpha}})$ as follows. First, we deduce from Watson's Lemma [24] that

$$\int_0^\infty u_e(x) e^{-\omega x^\alpha}\, \mathrm{d}x = \frac{1}{\alpha} \int_0^\infty t^{1/\alpha - 1} u_e(t^{1/\alpha}) e^{-\omega t}\, \mathrm{d}t = \mathcal{O}(\omega^{-\frac{d+1}{\alpha}})$$

when $\omega \to \infty$, because

$$t^{1/\alpha-1} u_e(t^{1/\alpha}) \sim t^{\frac{d+1}{\alpha}-1}, \qquad t \to 0$$

Next, for sufficiently large ω such that $x_k \omega^{-1/\alpha} < R$, we also have

$$u(x_k\, \omega^{-1/\alpha}) - u_d(x_k\, \omega^{-1/\alpha}) = \sum_{i=d}^{\infty} \frac{u^{(i)}(0)}{i!} x^i \omega^{-i/\alpha} = \mathcal{O}(\omega^{-\frac{d}{\alpha}}).$$

This proves the result.

Theorem 2.2 *Define the quadrature rule $Q[f; h_{a,j_1}]$ as in* (6)*, with n points and weights given by* (8)*. Then the approximation error behaves like*

$$I[f; h_{a,j_1}] - Q[f; h_{a,j_1}] = \mathcal{O}(\omega^{-2n-1}), \qquad \omega \to \infty.$$

Proof 2.2 *This follows immediately from Lemma 2.1 with $\alpha = 1$ and $u(x) = f(h_{a,j_1}(x)) h'_{a,j_1}(x)$. This function $u(x)$ is analytic at $x = 0$.*

Lemma 2.1 shows that high polynomial order d of the underlying quadrature rule translates into high asymptotic order, if the exponential decay is included into the weight function of the rule. Gaussian quadrature is a natural choice then, as it maximizes polynomial order. In that case, the error $\mathcal{O}(\omega^{-2n-1})$ should be compared to the error $\mathcal{O}(\omega^{-n-1})$ in (5), due to truncating the asymptotic expansion after n terms. Thus, using number of evaluations of f or its derivatives as a metric, the asymptotic order can be almost doubled at the same computational effort.

In addition, we make the following remarks:

- The result of Theorem 2.2 also holds for the other endpoint b. More generally, it holds for any point x where $g'(x) \neq 0$. At a stationary point, the function $h_{\xi,j}(p)$ is not analytic at $p = 0$ and Lemma 2.1 can not be invoked immediately.

- It is important to note that, unlike Filon-type quadrature, the quadrature rule $Q[f; h_{a,j_1}]$ is in general not exact when f is a polynomial. It is exact only if $f(h_{a,j_1}(p))h'_{a,j_1}(p)$ is a polynomial, of sufficiently small degree.
- Lemma 2.1 was proved for the specific case of Gaussian quadrature with $\alpha = 1$ in [13], based on the error expression for Gauss-Laguerre quadrature. The current method of proof is more general in two ways. Other values of α are useful in the presence of stationary points. Also, quadrature rules other than Gaussian ones can be used, for example Clenshaw-Curtis rules. The Lemma predicts what asymptotic order they will achieve.

2.2.2 Line integrals at stationary points

A similar reasoning can be applied to the integrals involving the stationary point $x = 0$. We recall the form of the asymptotic expansion

$$I[f; h_{\xi,j_m}] \sim \sum_{k=0}^{\infty} c_{m,k} \omega^{-\frac{k+1}{r}}, \qquad m = 1, 2, \quad \omega \to \infty,$$

where the coefficient $c_{m,k}$ depends on the values $f^{(j)}(0)$, $j = 0, \ldots, k$. Therefore, the truncation of the asymptotic expansion after n terms asymptotically behaves as

$$I[f; h_{\xi,j_m}] - \sum_{k=0}^{n-1} c_{m,k} \omega^{-\frac{k+1}{r}} = \mathcal{O}(\omega^{-\frac{n+1}{r}}), \qquad \omega \to \infty. \tag{10}$$

It turns out that the asymptotic order can be doubled in this case too, by considering a suitable Gauss-type quadrature rule. Let us consider first the single line integral $I[f; h_{\xi,j_2}]$. This integral is weakly singular, but the substitution $q = \sqrt[r]{p}$ yields a regular integral,

$$\begin{aligned} I[f; h_{\xi,j_2}] &= \frac{\mathrm{i}}{r} \int_0^{\infty} f(\sqrt[r]{\mathrm{i}p})(\mathrm{i}p)^{-\frac{r-1}{r}} \mathrm{e}^{-\omega p} \, \mathrm{d}p \\ &= \mathrm{i}^{\frac{1}{r}} \int_0^{\infty} f(q\sqrt[r]{\mathrm{i}}) \mathrm{e}^{-\omega q^r} \, \mathrm{d}q \\ &= \delta_r \int_0^{\infty} f(\delta_r t) \mathrm{e}^{-t^r} \, \mathrm{d}t, \end{aligned}$$

where $\delta_r = (\mathrm{i}/\omega)^{\frac{1}{r}}$ and we have used the change of variable $t^r = \omega q^r$ in the last integral. This is suitable for Gaussian quadrature with the non-standard weight function $w(t) = \mathrm{e}^{-t^r}$.Denote the points and weights of such a rule by w_k^{NS} and x_k^{NS}, and define

$$x_k(\omega) := \delta_r x_k^{NS} \qquad \text{and} \qquad w_k(\omega) := \delta_r w_k^{NS}. \tag{11}$$

The following theorem then follows from Lemma 2.1 with $\alpha = r$.

Theorem 2.3 *Define the quadrature rule* $Q[f;h_{\xi,j_2}]$ *with points and weights given by* (11)*. Then the error in approximating the steepest descent integral behaves like*

$$I[f;h_{\xi,j_2}] - Q[f;h_{\xi,j_2}] = \mathcal{O}(\omega^{-\frac{2n+1}{r}}), \qquad \omega \to \infty.$$

The asymptotic order is indeed approximately twice the order of (10). A similar result holds for $I[f;h_{\xi,j_1}]$.[1]

3 Gaussian quadrature rules with Freud-type weights

The application of deformation along paths of steepest descent leads us to the construction of Gaussian quadrature rules with respect to weight functions on $[0,\infty)$ of the form

$$w(x) = \mathrm{e}^{-x^r}. \tag{12}$$

The case $r = 1$ corresponds to the classical Gauss-Laguerre quadrature. For larger values of r we obtain the so-called Freud-type weights, which have been extensively studied in the literature (see for instance the reference [18]). In this section, we illustrate the properties of these rules when applied to oscillatory integrals, in view of the previous asymptotic results.

3.1 Construction of the quadrature rules

Define the linear functional

$$\mathcal{L}[f] := \int_0^\infty f(x)\mathrm{e}^{-x^r}\,\mathrm{d}x, \tag{13}$$

and the associated bilinear form

$$u(f,g) := \mathcal{L}[fg], \tag{14}$$

where fg is the pointwise product of $f(x)$ and $g(x)$. One can construct, analytically or numerically, a sequence of polynomials $p_n(x)$ that are orthogonal with respect to the bilinear form u, in the sense that

$$u(p_n,p_m) = \begin{cases} 0, & m \neq n \\ K_n \neq 0, & m = n, \end{cases}$$

and it is well known that the roots of $p_n(x)$ are the Gaussian quadrature points for the functional (13).

If the functional $\mathcal{L}[f]$ is positive definite, then the existence of the sequence $p_n(x)$ is a standard result in the general theory of orthogonal polynomials [3].

[1] Note that this result differs from the result in [13], where the use of generalized Gaussian quadrature is suggested. We point out that generalized Gaussian quadrature is not sufficient to fully resolve the weak singularity of the line integrals at the stationary point. This is hinted at in Remark 4.5 of [13], but should be emphasized here.

Moreover, the Gaussian nodes are real, distinct and contained in the interval of integration [3, 6, 9]. It is not hard to check that this is the case in the current setting, with the weight function $w(x) = \mathrm{e}^{-x^r}$.

The points and weights for Gaussian quadrature can be computed numerically in various ways. A crucial identity is the three-term recurrence relation satisfied by the sequence of (monic) orthogonal polynomials,

$$p_{n+1}(x) = (x - \alpha_n)p_n(x) - \beta_n p_{n-1}(x), \tag{15}$$

starting with initial values $p_{-1}(x) := 0$, $p_0(x) := 1$. The coefficients can be expressed in terms of the bilinear functional $u(f, g)$,

$$\begin{aligned} \alpha_n &= \frac{u(xp_n(x), p_n(x))}{u(p_n(x), p_n(x))}, \qquad n = 0, 1, 2, \ldots \\ \beta_n &= \frac{u(p_n(x), p_n(x))}{u(p_{n-1}(x), p_{n-1}(x))}, \qquad n = 1, 2, 3, \ldots, \end{aligned} \tag{16}$$

where β_0 is prescribed arbitrarily. Once these coefficients α_n and β_n are computed, the quadrature points and weights can be found by solving an eigenvalue problem associated with the recurrence (15) written in matrix-vector form [11, 9]. This approach was found to be numerically stable for the computation of Gaussian quadrature rules with Freud-type weights.

The recurrence coefficients α_n and β_n can be computed analytically by means of (16), though in most cases this process turns out to be numerically unstable and requires extended precision. The same comment applies to any expression involving Hankel determinants constructed from the moments of the weight function $w(x)$. Alternatively, the computation can be carried out in fixed double precision arithmetic using discretization methods [9]. This approach has been found to be satisfactory in the present context.

In order to evaluate steepest descent integrals, we transform the quadrature rules described above using (8) for the case of endpoint integrals and using (11) for the case of stationary point integrals. This step depends on the location of the endpoints and on the frequency parameter ω. The earlier steps, i.e. constructing the Gaussian rule with a Freud-type weight, have to be performed only once for each value of r and regardless of the value of ω.

3.2 Numerical examples

In this section we consider several numerical examples to illustrate the performance of the Gaussian quadrature. All computations have been carried out in Matlab (in fixed double precision), including the construction of the quadrature rules. The results have been compared with the direct evaluation of the integral given by Maple with extended precision to check accuracy.

Firstly, we illustrate the location of the nodes in the complex plane for different values of ω. Figures 2 and 3 show the cases $r = 3$ and $r = 4$ respectively on the interval $[a, b] = [-1, 1]$ with $\omega = 1, 10, 100$. Together with the nodes, the

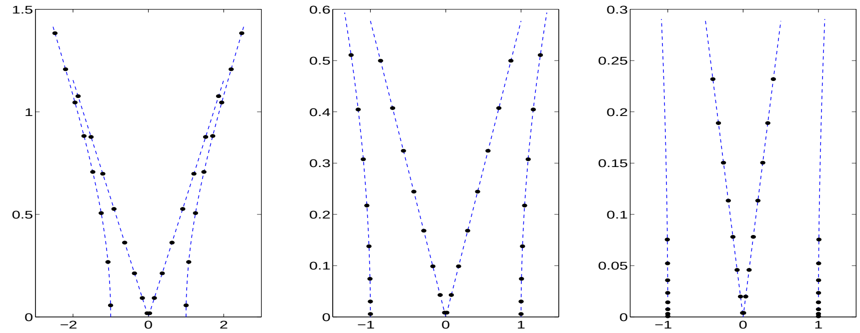

Figure 2: Location of the quadrature nodes for an oscillatory integral on $[-1,1]$ with $r=3$, corresponding to $\omega=1$ (left), $\omega=10$ (center) and $\omega=100$ (right). Eight points have been computed on each contour. The points are located on the paths of steepest descent (dashed line).

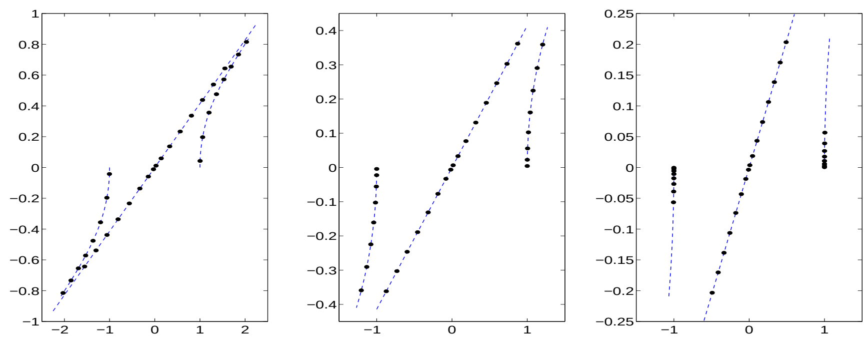

Figure 3: Location of the quadrature nodes for an oscillatory integral on $[-1,1]$ with $r=4$, corresponding to $\omega=1$ (left), $\omega=10$ (center) and $\omega=100$ (right). Eight points have been computed on each contour. The points are located on the paths of steepest descent (dashed line).

paths of steepest descent are plotted (dashed line). As can be observed, with increasing ω the nodes approach the endpoints of the interval of integration and the stationary point situated at the origin.

We consider the integral

$$I = \int_{-1}^{1} \sin(2x) e^{i\omega x^3} \, dx. \tag{17}$$

Figure 4 displays the absolute errors in the evaluation of (17) by a numerical steepest descent scheme for increasing ω. Taking into account Theorem 2.2 and

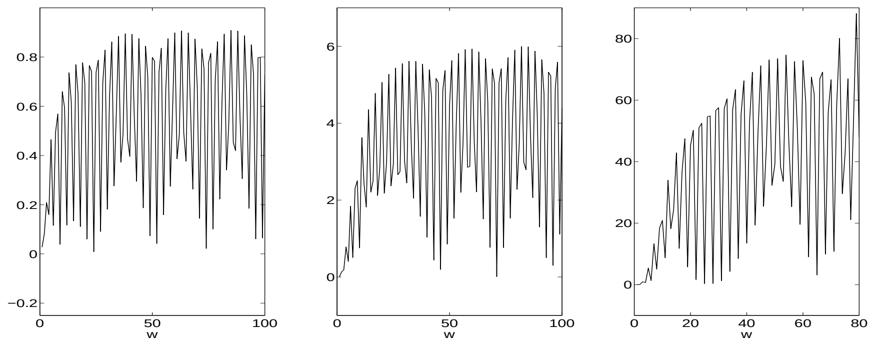

Figure 4: Absolute error in the computation of the integral (17). From left to right, results using $2+7$ nodes (scaled by ω^5), $3+10$ nodes (scaled by ω^7) and $4+13$ nodes (scaled by ω^9).

Theorem 2.3, we need a different number of points on the contours associated with the endpoints and on those involving the stationary point, in order to get similar asymptotic order of accuracy. For $r=3$ taking 2 points on the contours at $x=a$ and $x=b$ and 7 points on the contours at the origin ($2+7$ nodes for brevity) results in the overall estimate $\mathcal{O}(\omega^{-5})$ for the absolute error in the quadrature. Similarly, $3+10$ nodes yields $\mathcal{O}(\omega^{-7})$ and $4+13$ nodes produces $\mathcal{O}(\omega^{-9})$. In Figure 4 the absolute error is scaled by the corresponding power of ω.

Similar results are obtained for other values of r. Consider for example

$$I = \int_{-2}^{2} x \log(x+3) \mathrm{e}^{\mathrm{i}\omega x^4} \, \mathrm{d}x. \tag{18}$$

Again, we take different number of points to illustrate the asymptotic tendency in ω. In Figure 5 we use $1+6$ nodes, with a total estimate of $\mathcal{O}(\omega^{-3})$ and $2+10$, which gives $\mathcal{O}(\omega^{-5})$.

4 Asymptotically optimal quadrature rules

The use of Gaussian quadrature rules for the numerical evaluation of steepest descent integrals improves upon the asymptotic order of the asymptotic expansion using the same amount of information. One quickly sees however that the gain is only superficial in the presence of stationary points. Indeed, the method as described thus far in §2 and §3 requires the evaluation of two integrals at the stationary point. Using n quadrature points for both integrals requires $2n$ evaluations of the integrand in total. Using $2n$ terms in the asymptotic expansion for a fair comparison, rather than n, the error of both approaches carries the same asymptotic order.

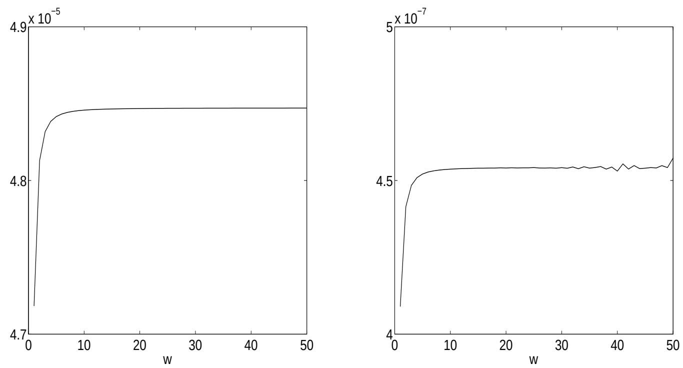

Figure 5: Absolute error in the computation of the integral (18). From left to right, results using $1+6$ nodes (scaled by ω^3) and $2+10$ nodes (scaled by ω^5).

Our results can be improved by observing that we may combine the two steepest descent integrals at the stationary point. That is, we will investigate the possibility of evaluating the difference of two integrals

$$I[f;h_{\xi,j_2}] - I[f;h_{\xi,j_1}] = \delta_r \int_0^\infty f(\delta_r t)\mathrm{e}^{-t^r}\,\mathrm{d}t - \lambda_r\delta_r \int_0^\infty f(\lambda_r\delta_r t)\mathrm{e}^{-t^r}\,\mathrm{d}t,$$

by a single quadrature rule. We have $\delta_r = (\mathrm{i}/\omega)^{\frac{1}{r}}$ as before and

$$\lambda_r = \mathrm{e}^{2\pi\mathrm{i}\lfloor\frac{r}{2}\rfloor\frac{1}{r}} = \begin{cases} \mathrm{e}^{\frac{2\pi\mathrm{i}s}{2s+1}}, & r = 2s+1, \\ -1, & r = 2s. \end{cases} \tag{19}$$

Hence, it becomes clear that the cases of even and odd r will lead to different results.

4.1 The case where r is even

For even values of $r = 2s$, the contribution of the stationary point is easily written as a single integral on $(-\infty,\infty)$,

$$\begin{aligned} I[f;h_{\xi,j_2}] - I[f;h_{\xi,j_1}] &= \delta_r \left[\int_0^\infty f(\delta_r t)\mathrm{e}^{-t^{2s}}\,\mathrm{d}t + \int_0^\infty f(-\delta_r t)\mathrm{e}^{-t^{2s}}\,\mathrm{d}t\right] \\ &= \delta_r \int_{-\infty}^\infty f(\delta_r t)\mathrm{e}^{-t^{2s}}\,\mathrm{d}t. \end{aligned}$$

In this case, the path is a straight line that makes an angle $\frac{\pi}{2r}$ with the real axis. This is illustrated for the case $r=2$ in the left panel of Figure 1. Weight functions of the form $\mathrm{e}^{-t^{2s}}$ on $(-\infty,\infty)$ are called Freud weights. Their treatment is not that different from that of the Freud-type weights that were described in §3. Note that the case $r=2$ corresponds to classical Gauss-Hermite quadrature.

We can extend the asymptotic results of Theorem 2.3 to this setting. To that end, consider the following small variation of Lemma 2.1.

Lemma 4.1 *Consider a positive number $\alpha \in \mathbb{R}$ and a quadrature rule with n points x_k and weights w_k, such that*

$$\int_{-\infty}^{\infty} x^m e^{-x^\alpha} \, \mathrm{d}x = \sum_{k=1}^{n} w_k x_k^m, \qquad m = 0, \ldots, d-1.$$

If $\int_{-\infty}^{\infty} u(x) e^{-\omega x^\alpha} \, \mathrm{d}x$ exists for $\omega \geq \omega_0$ and if u is analytic at $x = 0$, then it is true that

$$\int_{-\infty}^{\infty} u(x) e^{-\omega x^\alpha} \, \mathrm{d}x - \omega^{-1/\alpha} \sum_{k=1}^{n} w_k u(x_k \, \omega^{-1/\alpha}) = \mathcal{O}(\omega^{-\frac{d+1}{\alpha}}),$$

when $\omega \to \infty$.

The proof is entirely analogous to that of Lemma 2.1 and is omitted. This result shows that we are interested in quadrature rules corresponding to a functional of the form:

$$\mathcal{L}_H[f] := \int_{-\infty}^{\infty} f(x) \mathrm{e}^{-x^{2s}} \, \mathrm{d}x, \tag{20}$$

rather than (13). Letting x_k^H and w_k^H, $k = 1, \ldots, n$, be the Hermite-type Gaussian quadrature rule for (20), we set

$$x_k(\omega) := \delta_r x_k^H \qquad \text{and} \qquad w_k(\omega) := \delta_r w_k^H. \tag{21}$$

This is analogous to (11). We have the following result.

Theorem 4.2 *Define the quadrature rule $Q_H[f]$ with points and weights given by (21). Then the error in approximating the stationary point contribution for even $r = 2s$ behaves as*

$$(I[f; h_{\xi,j_2}] - I[f; h_{\xi,j_1}) - Q_H[f] = \mathcal{O}(\omega^{-\frac{2n+1}{r}}), \qquad \omega \to \infty.$$

Note that the Gaussian quadrature for (20) is guaranteed to exist because the functional is again positive definite.

4.2 The case where r is odd

When $r = 2s+1$ is odd, the setting is qualitatively very different. The combined path is the non-smooth union of two lines. This is illustrated in the right panel of Figure 1 for the case $r = 3$. In general, the two straight lines are at an angle of $\frac{r-1}{r}\pi$ to each other.

We recall that $\delta_r = (\mathrm{i}/\omega)^{\frac{1}{r}}$ and observe that

$$\lambda_r \delta_r = \varepsilon_s \mathrm{i}, \qquad \delta_r = \overline{\varepsilon_s} \mathrm{i},$$

where

$$\varepsilon_s = \left(\frac{\mathrm{e}^{\pi \mathrm{i} s}}{\omega}\right)^{\frac{1}{2s+1}}.$$

This allows us to cast the integral along the combined steepest descent contours in a more symmetric form,

$$I[f; h_{\xi,j_2}] - I[f; h_{\xi,j_1}]$$
$$= \mathrm{i}\left[-\varepsilon_s \int_0^\infty f(\varepsilon_s \mathrm{i}t)\mathrm{e}^{-t^{2s+1}}\,\mathrm{d}t + \overline{\varepsilon_s}\int_0^\infty f(\overline{\varepsilon_s}\mathrm{i}t)\mathrm{e}^{-t^{2s+1}}\,\mathrm{d}t\right]. \quad (22)$$

Let us define the linear functional

$$\mathcal{M}[f] = \int_\Gamma f(z)\mathrm{e}^{\mathrm{i}z^{2s+1}}\,\mathrm{d}z, \quad (23)$$

where Γ is the union of the two steepest descent paths at the stationary point. Similar to the functionals $\mathcal{L}[\cdot]$ and $\mathcal{L}_H[\cdot]$, this definition does not depend on ω. A suitable choice for Γ is obtained from the parameterization in (22) with $\omega = 1$. Let us assume next that a Gaussian quadrature rule exists for $\mathcal{M}[f]$, with quadrature points x_k^M and w_k^M. We then set

$$x_k(\omega) := \omega^{-\frac{1}{r}} x_k^M \qquad \text{and} \qquad w_k(\omega) := \omega^{-\frac{1}{r}} w_k^M, \quad (24)$$

such that the quadrature rule

$$Q_M[f] := \sum_{k=1}^n w_k(\omega) f(x_k(\omega))$$

is a reasonable approximation to (22). Analogues to Lemma 4.1 and Theorem 4.2 can be easily formulated. We omit the lemma and state the theorem.

Theorem 4.3 *Define the quadrature rule $Q_M[f]$ with points and weights given by* (24). *Then the error in approximating the stationary point contribution for odd $r = 2s+1$ behaves as*

$$(I[f; h_{\xi,j_2}] - I[f; h_{\xi,j_1}) - Q_M[f] = \mathcal{O}(\omega^{-\frac{2n+1}{r}}), \qquad \omega \to \infty.$$

It is not obvious however that a suitable Gaussian quadrature rule for $\mathcal{M}[f]$ does, indeed, exist, since we note that the functional $\mathcal{M}[f]$ is not positive definite. For example, in the case $r = 3$, we have $\mathcal{M}[x^2] = 0$. In fact, one can verify that the functional is indefinite for any odd value of r.

Orthogonal polynomials on the complex plane have been studied in literature. In most cases, the problems associated with functionals defined in the complex plane are avoided by considering orthogonality with respect to the bilinear form $v(f, g) = \mathcal{M}[f\bar{g}]$. This is more likely to lead to positive definite functionals, and in that case the general theory of orthogonal polynomials can

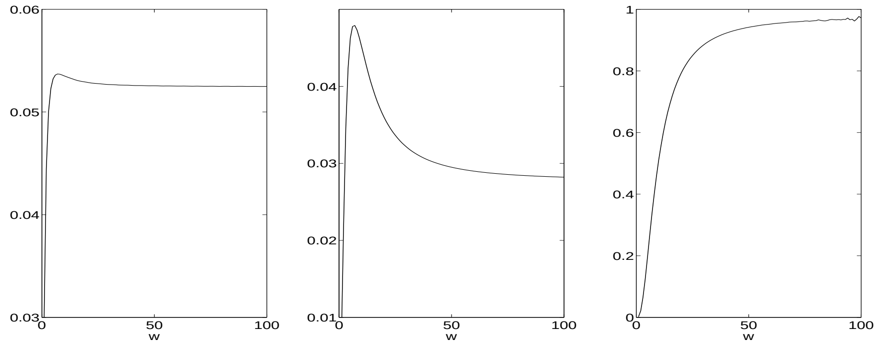

Figure 6: Absolute error in the computation of the integral (25). From left to right, results using $1+6$ nodes (scaled by ω^3), $2+10$ nodes (scaled by ω^5) and $3+14$ nodes (scaled by ω^7).

be applied. For example, orthogonality on equally spaced rays in the complex plane, a setting that is otherwise quite comparable to our setting, is considered in [19]. With the application to numerical integration in mind however, we are interested in the bilinear form $u(f,g) = \mathcal{M}[fg]$, which does not lead to a positive definite functional.

Nevertheless, suitable Gaussian quadrature rules exist and they can be computed numerically. The asymptotic order of Theorem 4.3 is observed in practice. In the following, we forego an existence proof of the orthogonal polynomials and the associated Gaussian quadrature rules in favour of a numerical illustration of their properties for the purposes of oscillatory quadrature. We do like to point out that the curves of quadrature points (as will be illustrated in Figures 7 and 8 below) can be determined asymptotically with a method of proof along the lines of that in [7]. This, incidentally, also proves existence of the orthogonal polynomials for large degree. These preliminary results are outside the scope of the current paper however and they are the subject of further study.

4.3 Numerical examples

All numerical results in this section have been computed in Matlab. The Gaussian quadrature rules corresponding to the functional $\mathcal{M}[f]$, with points x_k^M and weights w_k^M, have been precomputed in Maple. They need be computed once for each value of n and each value of r of interest, yet they are independent of ω. We note that, since $\mathcal{M}[fg] = \mathcal{M}[gf]$, the orthogonal polynomials satisfy the three-term recurrence relation (15), which greatly simplifies computations.

As an example, we consider the integral

$$I = \int_{-1}^{1} \cos(3x+2) \mathrm{e}^{\mathrm{i}\omega x^4} \, \mathrm{d}x. \tag{25}$$

This integral has a stationary point of order 3 at the origin. The paths of steepest descent through the origin combine into one straight line, enabling the use of Gauss-Hermite-type quadrature as described in §4.1. Figure 6 displays the absolute error using $1+6$ nodes, $2+6$ nodes and $3+14$ nodes. As before, by $1+6$ nodes we mean that 1 quadrature point is used along the steepest descent integrals corresponding to the endpoints and 6 points are used along the combined paths at the stationary point. This results, according to Theorem 2.2 and Theorem 4.2, in asymptotic errors of size $\mathcal{O}(\omega^{-3})$ and $\mathcal{O}(\omega^{-\frac{13}{4}})$ respectively. We therefore scaled the results by ω^3. The other choices achieve $\mathcal{O}(\omega^{-5})$ and $\mathcal{O}(\omega^{-7})$ absolute error and the results are scaled accordingly.

For odd values of r, Gaussian quadrature rules are used based on an indefinite functional. One consequence of this fact is that the quadrature points no longer lie on the paths of steepest descent.

The location of the nodes is shown in Figure 7 for $r=3$ and in Figure 8 for $r=5$. The figures also include the nodes for endpoint integrals at ± 1. The results are shown for different values of ω. The quadrature points for the stationary point contribution seem to lie on a smooth curve that is enclosed by the two paths of steepest descent. Similar results have been obtained for a wide range of n and r.

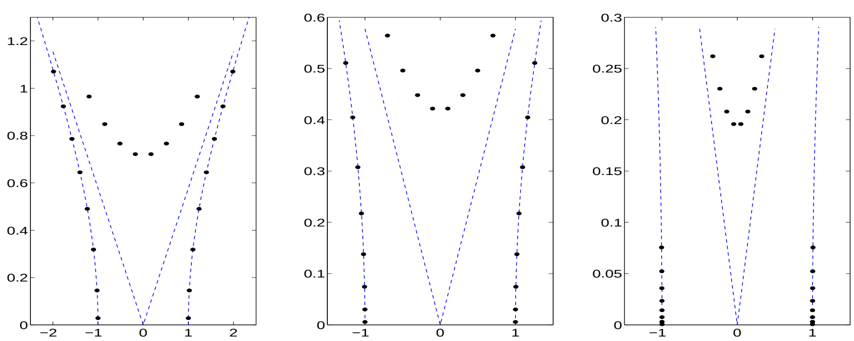

Figure 7: Location of the quadrature nodes for $r=3$ on $[-1,1]$, corresponding to $\omega=2$ (left), $\omega=10$ (center) and $\omega=100$ (right). Eight points have been computed for each integral.

We also present two examples of the performance of this indefinite quadrature rule, with the integrals:

$$\int_{-1}^{1} \frac{\cos(4x)}{x+3}\, \mathrm{e}^{\mathrm{i}\omega x^3}\, \mathrm{d}x, \qquad \int_{-1}^{1} \sqrt{x+6}\, \mathrm{e}^{\mathrm{i}\omega x^5}\, \mathrm{d}x. \tag{26}$$

The results are shown in Figures 9 and 10, again scaling with the appropriate power of the parameter ω.

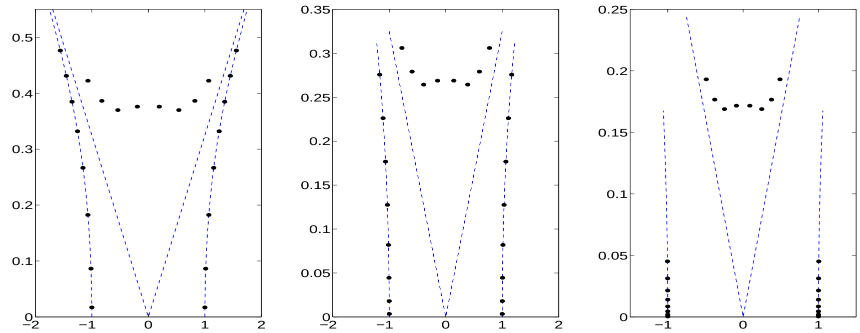

Figure 8: Location of the quadrature nodes for $r = 5$ on $[-1, 1]$, corresponding to $\omega = 2$ (left), $\omega = 10$ (center) and $\omega = 100$ (right). Eight points have been computed for each integral.

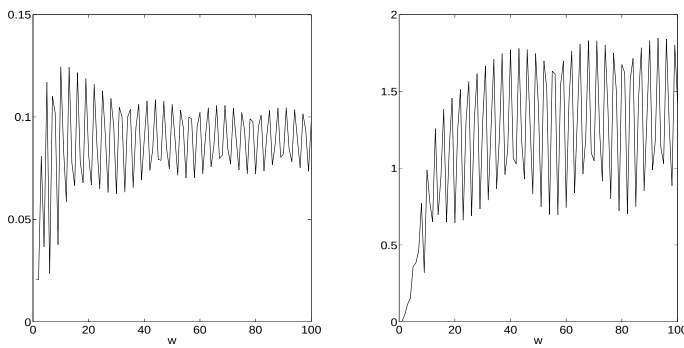

Figure 9: Absolute error in the computation of the first integral in (26). On the left, results using $2 + 7$ nodes (scaled by ω^5) and on the right using $3 + 10$ nodes (scaled by ω^7) .

5 More general oscillators $g(x)$

So far in this paper we have restricted our attention to integrals of the form (2) with $g(x) = x^r$, rather than the more general integral (1). In this section we will show that no new quadrature rules are required to cover the case of general oscillators $g(x)$. The evaluation of oscillatory integrals with any oscillator function $g(x)$ that is analytic on $[a, b]$ can be performed by the quadrature rules constructed in the previous sections.

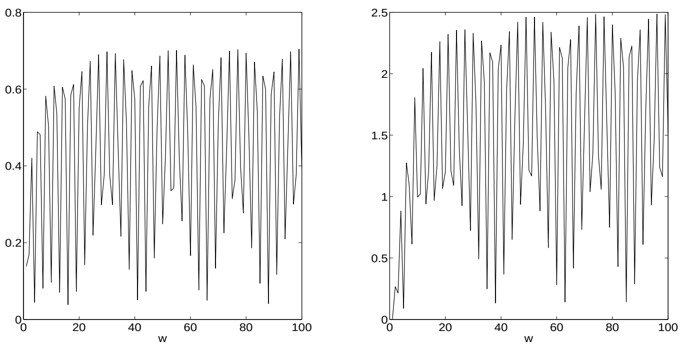

Figure 10: Absolute error in the computation of the second integral in (26). On the left, results using $1+7$ nodes (scaled by ω^3) and on the right using $2+12$ nodes (scaled by ω^5) .

5.1 A global substitution

Let us assume first for simplicity that the oscillator $g(x)$ has a single stationary point at $\xi = 0$ of order $r-1$ and that $\xi \in (a,b)$. In this setting, it is tempting to consider a substitution $x = u(y)$ that satisfies $g(u(y)) = y^r$. By our assumptions, the function $u(y)$ is guaranteed to exist and it is invertible on the interval $[a,b]$. With this approach, we obtain

$$\int_{u^{-1}(a)}^{u^{-1}(b)} f(u(y))u'(y)\mathrm{e}^{\mathrm{i}\omega y^r}\,\mathrm{d}y, \tag{27}$$

and the problem is reduced to the integral previously studied. Integral (27) can be evaluated efficiently after deforming the integration contour onto the paths of steepest descent. Note that the substitution is independent of ω, so all asymptotic error estimates continue to hold.

5.2 Localizing the computations

The substitution $x = u(y)$ however may be cumbersome to construct in practice, especially away from the stationary point $x = \xi$. A more practical formulation is found by immediately deforming onto the paths of steepest descent with respect to the oscillator $g(x)$. The result is mathematically equivalent to the steepest descent integrals one would obtain after the global substitution described above, in the case of a single stationary point. Yet, it requires only local computations in practice. Moreover, this approach is easily generalized to the case of multiple stationary points.

We consider first the endpoints. The general form of equation (3) to solve for the paths of steepest descent at $x = a$ or $x = b$ becomes

$$g(h_x(p)) = g(x) + \mathrm{i}p. \tag{28}$$

This leads to line integrals of the form

$$I[f;h_x] = \mathrm{e}^{\mathrm{i}\omega g(x)} \int_0^\infty f(h_x(p))h_x'(p)\mathrm{e}^{-\omega p}\,\mathrm{d}p.$$

They are suitable for Gauss-Laguerre quadrature as before. Note that equation (28) can no longer be solved explicitly, as it is comparable to computing the inverse of g. A numerical approach is described in [13] based on rapidly convergent Newton–Raphson iterations. The derivative $h_x'(p)$ can be obtained in terms of $h_x(p)$ by differentiating (28), which yields

$$h_x'(p) = \frac{\mathrm{i}}{g'(h_x(p))}.$$

At the stationary point ξ, we deform onto the paths of steepest descent that satisfy

$$g(h_{\xi,j}(q)) = g(\xi) + \mathrm{i}q^r. \tag{29}$$

This equation has r analytic solutions when q is sufficiently small. As before, there are only two relevant solutions h_{ξ,j_m}, $m = 1, 2$. They lead to two line integrals of the form

$$I[f;h_{\xi,j_m}] = \mathrm{e}^{\mathrm{i}\omega g(\xi)^r} \int_0^\infty f(h_{\xi,j_m}(q))h_{\xi,j_m}'(q)\mathrm{e}^{-\omega q^r}\,\mathrm{d}q$$

The derivatives are given by

$$h_{\xi,j_m}'(q) = \mathrm{i}rq^{r-1}\frac{1}{g'(h_{\xi,j_m}(q))}.$$

This approach is comparable to performing the substitution $g(x) = y^r$ locally at the point $x = \xi$. We note that the quadrature rules that were constructed earlier in this paper can again be applied. The two line integrals at the stationary point can be combined. The sole difference compared to the case $g(x) = x^r$ is that the paths $h_{\xi,j}(q)$ are no longer straight lines.

As an example, consider the integral

$$I = \int_{-1}^1 [\cos(x) + \sin(x)]\mathrm{e}^{\mathrm{i}\omega(x^4+4x^3)}\,\mathrm{d}x.$$

The oscillator $g(x) = x^4 + 4x^3$ has a stationary point of order 2 at $\xi = 0$. We apply a Gaussian quadrature rule with $2 + 7$ nodes, i.e., 2 point at both endpoints and 7 points for the combined stationary point contribution. This yields an absolute error of $\mathcal{O}(\omega^{-5})$. The results are shown in Figure 11. Note that the quadrature points corresponding to the Gauss-Laguerre quadrature lie on the paths of steepest descent. The other points lie in the interior between the two paths at the stationary point. For comparison, the paths of steepest descent corrsponding to $g(x) = x^3$ are also shown in the right panel of the figure. The paths that correspond to $g(x) = x^4 + 4x^3$ behave qualitatively similar near $\xi = 0$, but they are curved.

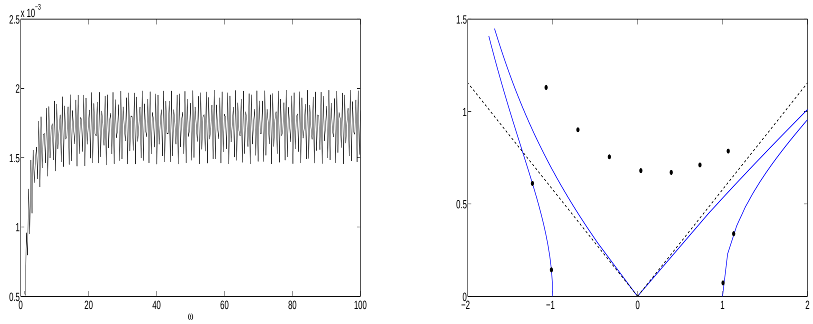

Figure 11: Absolute error in the evaluation of $\int_{-1}^{1}[\sin(x)+\cos(x)]e^{i\omega(x^4+4x^3)}\,dx$. We have used $2+7$ quadrature nodes. The left panel shows the absolute error, scaled by ω^5 (at $\omega = 100$, the error is 1.8×10^{-13}). The right panel shows the paths of steepest descent (solid lines), the paths of steepest descent for $g(x) = x^3$ (dashed lines) and the location of the quadrature points corresponding to $\omega = 1$.

6 Acknowledgements

The authors would like to acknowledge useful discussions with A. Iserles (DAMTP, University of Cambridge), A. Kuijlaars (Katholieke Universiteit Leuven), D. Levin (University of Tel Aviv), F. Marcellán (University Carlos III de Madrid) and B. Adcock (DAMTP, University of Cambridge). The first author acknowledges financial support from the programme of postdoctoral grants of the Spanish Ministry of Education and Science. The second author is a Postdoctoral Fellow of the Research Foundation - Flanders (FWO).

References

[1] N. Bleistein and R. A. Handelsman. *Asymptotic expansions of integrals.* Dover Pubns, 1986.

[2] S. N. Chandler-Wilde and D. C. Hothersall. Efficient calculation of the Green function for acoustic propagation above a homogeneous impedance plane. *J. Sound Vibration*, 180(5):705–724, 1995.

[3] T.S. Chihara. *An introduction to orthogonal polynomials.* Gordon and Breach, 1978.

[4] R. Cools. Constructing cubature formulae: The science behind the art. *Acta Numer.*, 6:1–54, 1997.

[5] K. T. R. Davies, M. R. Strayer, and G. D. White. Complex-plane methods for evaluating highly oscillatory integrals in nuclear physics. I. *J. Phys. G: Nucl. Phys.*, 14(7):961–972, 1988.

[6] P. J. Davis and P. Rabinowitz. *Methods of numerical integration*. Academic Press, 1984.

[7] M. Duits and A. B. J. Kuijlaars. Painlev I asymptotics for orthogonal polynomials with respect to a varying quadratic weight. *Nonlinearity*, 19:2211–2245, 2006.

[8] J. Franklin and B. Friedman. A convergent asymptotic representation for integrals. *Proc. Cambridge Philos. Soc.*, 53:612–619, 1957.

[9] W. Gautschi. *Orthogonal polynomials. Computation and approximation*. Oxford University Press, 2004.

[10] A. Gil, J. Segura, and N. M. Temme. *Numerical methods for special functions*. SIAM, 2007.

[11] G. H. Golub and J. H. Welsch. Calculation of Gauss quadrature rules. *Math. Comp.*, 23(106):221–230, 1969.

[12] D. Huybrechs and S. Olver. *Highly Oscillatory Problems: Computation, Theory and Applications*, chapter Oscillatory integrals. Cambridge Univ. Press, 2008.

[13] D. Huybrechs and S. Vandewalle. On the evaluation of highly oscillatory integrals by analytic continuation. *SIAM J. Numer. Anal.*, 44(3):1026–1048, 2006.

[14] D. Huybrechs and S. Vandewalle. The construction of cubature rules for multivariate highly oscillatory integrals. *Math. Comp.*, 76(260):1955–1980, 2007.

[15] A. Iserles and S.P. Nørsett. On quadrature methods for highly oscillatory integrals and their implementation. *BIT*, 44:755–772, 2004.

[16] D. S. Jones. Asymptotic behavior of integrals. *SIAM Rev.*, 14(2):286–317, 1972.

[17] D. Levin. Procedure for computing one- and two-dimensional integrals of functions with rapid irregular oscillations. *Math. Comp.*, 38(158):531–538, 1982.

[18] E. Levin and D. Lubinsky. *Orthogonal Polynomials for Exponential Weights*. Springer, New York, 2001.

[19] G. V. Milovanovic. A class of polynomials orthogonal on the radial rays in the complex plane. *J. Math. Anal. Appl.*, 206:121–139, 1997.

[20] F.W.J. Olver. *Asymptotics and special functions*. Academic Press, San Diego, 1974.

[21] S. Olver. Moment-free numerical integration of highly oscillatory functions. *IMA J. Num. Anal.*, 26(2):213–227, 2006.

[22] E. Stein. *Harmonic analysis: Real-variable methods, orthogonality and oscillatory integrals.* Princeton University Press, Princeton, New Jersey, 1993.

[23] J. A. C. Weideman and L. N. Trefethen. Parabolic and hyperbolic contours for computing the Bromwich integral. *Math. Comp.*, 76:1341–1356, 2007.

[24] R. Wong. *Asymptotic approximations of integrals.* Academic Press, 1989.